*Carbohydrate Research*, 207 (1990) 221–235
Elsevier Science Publishers B.V., Amsterdam



# Conformational analysis of inulobiose by molecular mechanics*

Tomas M. Calub, Andrew L. Waterhouse†
*Department of Chemistry, Tulane University, New Orleans, Louisiana 70118 (USA)*

and Alfred D. French
*Southern Regional Research Center, United States Department of Agriculture, P. O. Box 19687, New Orleans, Louisiana, 70179 (USA)*

(Received December 19th, 1989; accepted in revised form, April 13th, 1990)

ABSTRACT

Conformational energies for inulobiose [β-D-fructofuranosyl-(2→1)-β-D-fructofuranoside], a model for inulin, were computed with the molecular mechanics program MMP2(85). The torsion angles of the three linkage bonds were driven in 20° increments, and the steric energy of all other parameters was minimized. The linkage torsion angles defined by C-1′-C-2′-O-C-1 ($\varphi$) and O-C-1-C-2-O-2 ($\omega$) have minima at +60° and −60°, respectively, regardless of side group orientation; accessible minima exist at other staggered conformations. The torsion angle at the central bond C-2′-O-1-C-1-C-2 ($\psi$) was approximately 180° in all the low-energy conformers. This appears to be generally true for rings linked by three bonds. The fructofuranose rings initially had low-energy ${}^{4}_{1}T$ conformations (angle of pseudorotation, $\varphi_2$ = 265°) that were retained except when the linkage conformations created severe inter-residue conflicts. In those cases, almost all puckerings of the furanose rings were found.

## INTRODUCTION

Inulobiose (Fig. 1) is the simplest among the homologous series of β-(2→1)-linked fructofuranoses. It can be obtained from the controlled acid hydrolysis of the homologous polysaccharide, inulin[1], and it can also be prepared by enzymic synthesis from fructose[2] and from raffinose, in the presence of fructose[3]. The inulobiose moiety is a component of 1-kestose and nystose which are ingredients of a low-calorie sweetener[4]. Aqueous solutions of inulin have a medical use as they are used to measure the efficiency of glomerular filtration in kidneys[5]. Other uses of fructans have been compiled in a recent review[6].

Fructofuranose rings linked by three bonds are a characteristic of fructans such as inulin and levan, the β-(2→6)-linked fructan, but little is known about the likely conformations of these three-bond linkages. A single-crystal diffraction study has been performed for 1-kestose[7], and the rough outlines of accessible conformations for inulin were previously described[8]. Previous modeling and X-ray powder diffraction work[9] on

* Paper 2 of a series: Conformational Analysis of Fructans.
† To whom correspondence should be addressed.

0008-6215/90/$ 03.50 

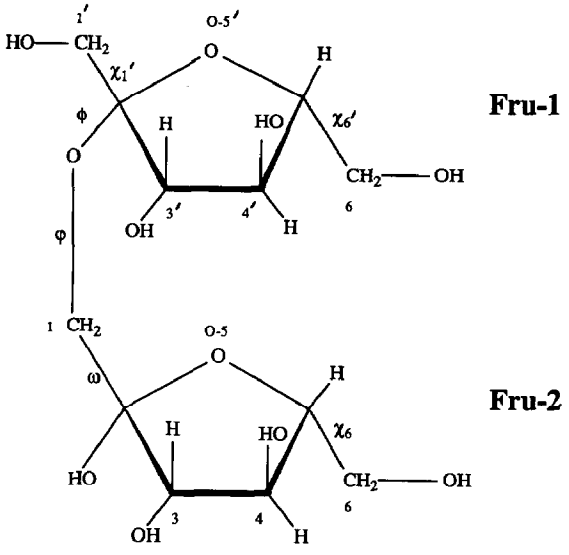


1

Fig. 1. Inulobiose (1). The atom numbering is based on 1-kestose. $\varphi$ = C-1′–C-2′–O–C-1; $\psi$ = C-2′–O–C-1–C-2; $\omega$ = O–C-1–C-2–O-2; chi-1′ = O-1′–C-1′–C-2′–O; chi-6 = O-5–C-5–C-6–O-6; chi-6′ = O-5′–C–5′–C-6′–O-6′.

the preferred conformations of inulin proposed a five-fold helical structure that could be either right- or left-handed. There is some doubt about these helical characteristics, since the repeat distance was based on a strong reflection at 10.6 Å. In most fiber diffraction patterns, the reflection corresponding to the fiber repeat distances is either absent or very, very weak.

In order to learn more about the likely conformations in inulobiose linkages found as constituents in larger molecules, we have modeled the isolated molecule of inulobiose. While comparisons with experimental studies on the disaccharide are usually beneficial, prospects for useful information are poor in this case. This is because reducing fructose moieties usually adopt the pyranoid ring rather than the furanoid ring of the residues in fructan polymers[10]. Therefore, this work stands without experimental corroboration except for comparison with the X-ray study of 1-kestose. However, we except that these results will aid in projects underway, such as the crystallographic study of nystose and a structural determination of 1-kestose in solution by n.m.r. spectroscopy[11].

In this work, we attempted to determine the steric energy of inulobiose for different values of the torsion angles for the three linkage bonds: $\varphi$, $\psi$, and $\omega$. The conformations of the three primary alcohol groups not involved in the linkage also affect the energy values, as do the conformations of the fructofuranose rings themselves. Because of the many degrees of freedom in this system and computational time restraints, some compromises in the extent of the study were necessary.

Optimization at each 20° step for two (linkage) torsion angles required about 3.5 c.p.u. days on the MicroVax II computer available for this work. Complete concurrent analysis of a third torsion angle would increase the time by a factor of 18 to 63 c.p.u. days. Concurrent consideration of the three primary alcohol groups, again with full optimization at each 20° increment, would multiply the 63 days by $18^3$, or $\sim 370\,000$ c.p.u. days. Analysis of a variety of initial ring geometries would increase the time further. Ultimately, we were able to analyze two of the linkage torsion angles at a time, with various combinations of the third linkage angle and the three staggered forms of the hydroxymethyl side groups that form the chi angles (Fig. 1). Although we started with analyses of $\varphi$ and $\psi$, it became apparent that $\psi$ could only assume a narrow range, and it was therefore left in that range while $\varphi$ and $\omega$ were varied.

## CONFORMATIONAL AND COMPUTATIONAL DETAILS

The five-membered furanose ring is generally nonplanar. It can be puckered in an envelope ($E$) form with four atoms in a plane and the fifth atom out; or in a twist ($T$) form with two adjacent atoms displaced on opposite sides of a plane through the three atoms[12]. Atom numbers, written as subscripts or superscripts, indicate whether these atoms are displaced above or below the plane. All possible conformations of the furanose ring can be systematically related by the use of the pseudorotational wheel (Fig. 2) similar to one that is used extensively for aldofuranose descriptions[10,13]. Positions on the wheel can be indicated with $E/T$ notation or the corresponding phase of pseudorotation, $\varphi_2$, calculated according to Cremer and Pople[14], and used in the following section.

The analysis of **1** as a model for 1-kestose and inulin was started by creating an inulobiose model using the most favored ring conformation, ${}^{4}_{3}T$ ($\varphi_2 = 265°$) of β-D-

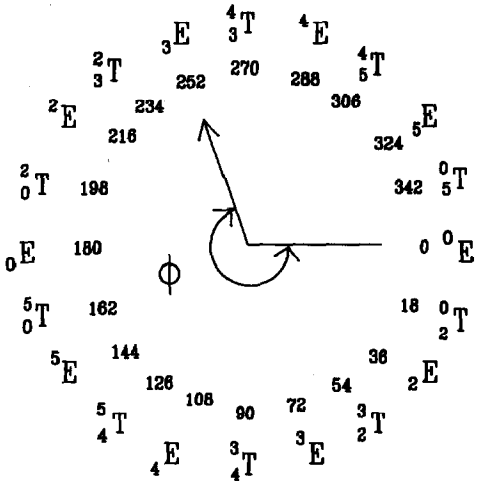


Fig. 2. Conformational wheel for the fructofuranose ring relating the Cremer–Pople angle of pseudorotation, $\varphi_2$, and the furanose ring conformation.

fructofuranose[13]. No attempt was made to search for any other favorable ring conformations after the model was created, nor was any attempt made to optimize the structure before the torsion angle analyses were carried out.

Analyses were carried out by driving two of the above torsion angles at a time using MMP2(85), and each optimization was terminated when $\Delta E$ between the current optimization and the previous optimization was less than or equal to $0.0008N$, $N$ being the number of atoms in the molecule. This value is 10 times higher than the default value in the program, and it allowed the analysis to finish in half the time. As the calculations proceed, all other internal coordinates (bond lengths, angles, and torsion angles) will vary to lower steric energy, but steric energy barriers, which may lie between the existing form and a lower energy form, will not be crossed. For this reason, a modified version of MMP2(85) was used which has a new torsion angle driver (option -2). This version executes each new optimization using the initial input residue geometry, changing only the driven torsion angle for each succeeding calculation[15]. With the standard driver (option -1), each optimization begins with the structure from the previous angle optimization. In high-energy conformations, deformable structures can be distorted into local minima (*i.e.*, boat forms in six-membered rings) that are best for the high-energy conformation. Subsequent optimizations at low-energy points will fail to return the deformed geometric feature to a low-energy form. Thus, the geometry from the previous optimization is not always suitable as input for the next calculation.

The MMP2(85) program was chosen primarily because it incorporates distance and energetic compensation for anomeric effects[16]. This program does not fully account for hydrogen bond energies, but that can be considered an advantage since the model is an isolated molecule. If full energetic compensation for hydrogen bonding were realized, models with intramolecular hydrogen bonds would dominate the modeling results even though both intra- and inter-molecular hydrogen bonds are typical of carbohydrates in both solution and in the solid states.

The model of **1** was initially analyzed by driving the torsion angles $\varphi$ and $\psi$ to determine the combinations that give low values of steric energy. Nine starting structures of **1** were created with all combinations of the staggered forms of chi-6 and chi-6′. By driving $\varphi$ and $\psi$ angles through a full 360° at 20° increments, 18 by 18 grids were produced for each of the runs A1–A9, but only A1 is tabulated below (Tables I and III).

Three $\varphi$–$\omega$ runs were carried out on two related hydrocarbons, dicyclopentylethane (**2**), run B1 and 1′,1″-dimethyldicyclopentylethane (**3**), runs B2 and B3, at selected starting $\psi$ angles and ring conformations to compare the final $\psi$ angle and energy. The initial ring form was derived by minimizing the steric energy of cyclopentane and was an envelope form with the out-of-plane atom at the linkage (Tables I–III).

The least energetic angles of $\varphi$, chi-6, and chi-6′ (160°, −60°, and −60°, respectively) from the $\varphi$–$\psi$ analyses of **1** (A runs) were used in the next analyses for $\varphi$, $\omega$ and chi-1′ of **1**. Input structures for runs C1–C3 varied the initial settings of the torsion angle chi-1′ = +60°, −60°, and 180°, respectively, the three staggered forms.

Two other $\varphi$–$\omega$ searches were run using the best $\psi$, 160° and best chi-1′, +60°, found in runs C1–C3 and setting chi-6 and chi-6′ both to 60° and 180°, giving runs C4

TABLE I

Initial torsion angle settings for all input structures[a].

| *Run* | *Torsion angle* | | | | | |
|---|---|---|---|---|---|---|
| | $\varphi$ | $\psi$ | $\omega$ | *chi-1'* | *chi-6* | *chi-6'* |
| A1 | D | D | 180.00 | 180.00 | −60.00 | −60.00 |
| B1 | D | 180.00 | D | | | |
| B2 | D | 180.00 | D | | | |
| B3 | D | 60.00 | D | | | |
| C1 | D | 160.00 | D | 180.00 | −60.00 | −60.00 |
| C2 | D | 160.00 | D | −60.00 | −60.00 | −60.00 |
| C3 | D | 160.00 | D | 60.00 | −60.00 | −60.00 |
| C4 | D | 160.00 | D | 60.00 | 60.00 | 60.00 |
| C5 | D | 160.00 | D | 60.00 | 180.00 | 180.00 |
| C6 | D | 90.00 | D | 60.00 | −60.00 | −60.00 |

[a] "D" indicates that the torsion angle was driven.

TABLE II

Average $\psi$ values for each run.

| *Run* | *Average* $\psi$ (°) | *Standard deviation* (°) |
|---|---|---|
| B1 | 179.95 | 2.44 |
| B2 | 179.36 | 3.69 |
| B3 | 103.33 | 34.08 |
| C1 | 165.33 | 2.84 |
| C2 | 165.66 | 3.26 |
| C3 | 165.02 | 3.02 |
| C4 | 160.43 | 3.50 |
| C5 | 160.77 | 3.69 |

TABLE III

Torsion angle settings of each of the lowest energy structures found in each run.

| *Run* | *Torsion angle* | | | | | | |
|---|---|---|---|---|---|---|---|
| | $\varphi$ | $\psi$ | $\omega$ | *chi-1'* | *chi-6* | *chi-6'* | *Energy* |
| A1 | 60.00[a] | 160.00* | −85.74 | 177.40 | −59.41 | −55.72 | 39.54 |
| B1 | −60.00[a] | 175.90 | −60.00* | | | | |
| B2 | −60.00[a] | 173.43 | −60.00* | | | | |
| B3 | −60.00[a] | 173.67 | −60.00* | | | | |
| C1 | 60.00[a] | 163.83 | −60.00* | 178.48 | −60.53 | −59.09 | 37.16 |
| C2 | 60.00[a] | 164.86 | −60.00* | −74.38 | −60.83 | −59.62 | 36.65 |
| C3 | 60.00[a] | 166.31 | −60.00* | 55.76 | −61.65 | −58.52 | 34.91 |
| C4 | 60.00[a] | 162.49 | −60.00* | 56.27 | 61.77 | 62.05 | 38.11 |
| C5 | 60.00[a] | 161.47 | −60.00* | 56.31 | 171.36 | 171.93 | 38.05 |
| C6 | 40.00[a] | 81.00 | −80.00* | 59.37 | −60.57 | −73.15 | 38.66 |

[a] Denotes that the angle was driven and thus was not allowed to relax.

TABLE IV

Torsion angles of the fully relaxed inulobiose models starting from the minimum for each run in Table III.

| *Run* | *Torsion angle* | | | | | | |
|---|---|---|---|---|---|---|---|
| | *φ* | *ψ* | *ω* | *chi-1'* | *chi-6* | *chi-6'* | *Energy* |
| C1 | 53.21 | 164.34 | −57.89 | 177.83 | −60.53 | −58.61 | 36.76 |
| C2 | 54.59 | 165.70 | −57.61 | −74.53 | −60.75 | −59.26 | 36.34 |
| C3 | 51.59 | 168.83 | −58.20 | 58.22 | −60.84 | −58.67 | 34.44 |
| C4 | 51.61 | 165.45 | −59.42 | 56.27 | −61.77 | 62.05 | 38.11 |
| C5 | 50.61 | 164.54 | −59.03 | 56.31 | 171.36 | 171.93 | 38.05 |
| C6 | 42.02 | 79.13 | −79.34 | 58.80 | −60.59 | −72.75 | 38.54 |
| 1-KESTOSE[a] | 88.84 | −162.34 | 42.54 | 179.19 | 64.54 | 64.21 | 59.16[b] |

[a] Values were obtained from crystallographic data[7]. [b] The value was obtained by calculating the energy of the inulobiose fragment of 1-kestose using the carbon and oxygen coordinates but allowing the hydrogens to find their optimum position.

TABLE V

*φ*–*ω* Grid indicating the C run from which the minimum was obtained at each angle combination[a]

*The low-energy C run for each φ/ω combination*

| | | | | | | | | | | | | | | | | | |
|---|---|---|---|---|---|---|---|---|---|---|---|---|---|---|---|---|---|
| C3 | C3 | C3 | C3 | C3 | C3 | C2 | C2 | C3 | C3 | C2 | C2 | C2 | C3 | C2 | C3 | C3 | C3 | 160 |
| C3 | C3 | C3 | C3 | C3 | C2 | C2 | C2 | C3 | C3 | C3 | C2 | C2 | C2 | C3 | C3 | C3 | C3 | 140 |
| C3 | C3 | C3 | C3 | C3 | C2 | C2 | C2 | C3 | C3 | C3 | C2 | C2 | C2 | C2 | C5 | C3 | C3 | 120 |
| C3 | C3 | C3 | C3 | C3 | C3 | C2 | C2 | C3 | C3 | C3 | C2 | C2 | C2 | C2 | C5 | C3 | C3 | 100 |
| C5 | C3 | C3 | C3 | C3 | C3 | C2 | C3 | C3 | C3 | C3 | C5 | C2 | C2 | C2 | C5 | C3 | C5 | 80 |
| C3 | C5 | C3 | C3 | C2 | C2 | C2 | C2 | C3 | C3 | C3 | C5 | C5 | C4 | C2 | C2 | C3 | C3 | 60 |
| C3 | C3 | C3 | C3 | C2 | C2 | C2 | C2 | C3 | C3 | C3 | C3 | C5 | C5 | C2 | C2 | C2 | C3 | 40 |
| C3 | C3 | C3 | C2 | C3 | C2 | C2 | C2 | C3 | C3 | C3 | C3 | C5 | C4 | C2 | C5 | C2 | C3 | 20 |
| C3 | C3 | C3 | C3 | C3 | C2 | C2 | C2 | C3 | C3 | C3 | C3 | C3 | C3 | C3 | C5 | C5 | C4 | 0 |
| C3 | C3 | C3 | C3 | C2 | C2 | C2 | C2 | C3 | C3 | C3 | C3 | C3 | C3 | C3 | C5 | C5 | C4 | −20 |
| C3 | C3 | C3 | C3 | C2 | C2 | C2 | C2 | C3 | C3 | C3 | C3 | C3 | C3 | C3 | C3 | C5 | C5 | −40 |
| C3 | C3 | C3 | C5 | C2 | C2 | C2 | C2 | C2 | C3 | C3 | C3 | C3 | C3 | C3 | C3 | C5 | C5 | −60 |
| C3 | C3 | C3 | C3 | C3 | C2 | C2 | C2 | C2 | C1 | C3 | C3 | C3 | C3 | C3 | C3 | C3 | C4 | −80 |
| C3 | C3 | C3 | C3 | C3 | C2 | C2 | C2 | C2 | C2 | C3 | C3 | C3 | C3 | C3 | C3 | C3 | C3 | −100 |
| C3 | C3 | C3 | C4 | C3 | C2 | C2 | C2 | C2 | C2 | C2 | C4 | C3 | C2 | C2 | C3 | C3 | C3 | −120 |
| C3 | C3 | C3 | C3 | C3 | C3 | C2 | C2 | C2 | C2 | C2 | C3 | C4 | C3 | C2 | C3 | C3 | C3 | −140 |
| C3 | C3 | C3 | C4 | C3 | C3 | C2 | C2 | C2 | C2 | C2 | C2 | C3 | C4 | C2 | C3 | C3 | C3 | −160 |
| C3 | C3 | C3 | C3 | C3 | C3 | C2 | C2 | C3 | C3 | C3 | C2 | C2 | C3 | C2 | C3 | C3 | C3 | −180 |
| | | | | | | | | | | | | | | | | | | *ω* |
| — | — | — | — | — | — | — | — | — | | | | | | | | | | |
| 1 | 1 | 1 | 1 | 1 | | | | | | | | | | 1 | 1 | 1 | 1 | |
| 8 | 6 | 4 | 2 | 0 | 8 | 6 | 4 | 2 | | 2 | 4 | 6 | 8 | 0 | 2 | 4 | 6 | |
| 0 | 0 | 0 | 0 | 0 | 0 | 0 | 0 | 0 | 0 | 0 | 0 | 0 | 0 | 0 | 0 | 0 | 0 | |
| | | | | | | | | | | *φ* | | | | | | | | |

[a] C1 = 0.31%; C2 = 30.56%; C3 = 59.26%; C4 = 3.09%; C5 = 6.79%.

TABLE VI

Torsion angles of the fully relaxed form of C3 as optimized using different molecular modeling programs[a]

| *Method* | *Angle* | | | | | |
|---|---|---|---|---|---|---|
| | $\varphi$ | $\psi$ | $\omega$ | chi-1′ | chi-6 | chi-6′ |
| MMP2(85)[a] | 51.59 | 163.83 | −58.20 | −60.84 | −58.67 | 58.22 |
| MMP2(87) | 48.64 | 164.84 | −55.12 | −54.69 | −56.10 | 62.26 |
| MM3 | 46.72 | 169.34 | −55.29 | −60.00 | −57.87 | 67.61 |
| AM1 | 49.13 | 169.21 | −47.87 | −63.73 | −56.95 | 40.55 |

[a] The starting structure for the other methods.

and C5. Run C6 was carried out using the input structure for run C3, but $\psi$ was started at 90° and allowed to find its low-energy point (Table I).

The steric energies for each set of calculations (A1–A9 and C1–C5) were then extracted, and, using these data, input data files were created using the utility program MAPREP[15] for the contour plotting program, SURFER*, to create energy maps such as those in Fig. 4 and 6. Only structures within 10 kcal·mol$^{-1}$ of the minimum of each run were included in the contour map of that run. The linkage and side-group torsion angles from the low-energy structure of each run is listed in Table III, and these structures from the C runs were reoptimized without any geometric constraints. The same parameters from these calculations are listed in Table IV and compared with the crystallographic data[7].

This fully relaxed geometry from C3 was used as the input structure for comparison with the optimum structure found by other programs: MMP2(87), MM3, and MOPAC(AM1). The results are listed in Table VI.

Changes in the Cremer–Pople $\varphi_2$ values as a function of the linkage torsion angles $\varphi$ and $\omega$ were monitored, and contour maps from these analyses were plotted. Finally, changes in $\psi$ as a function of the $\varphi$, $\omega$, chi-1′, chi-6, and chi-6′ angles were also checked for all the B and C runs.

## RESULTS AND DISCUSSION

*Understanding $\varphi$–$\psi$–$\omega$ variation space.* — Initially, we varied the two torsion angles typically studied in conformational analysis of disaccharides, $\varphi$ and $\psi$ (runs A1–A9 used different initial orientations of two primary alcohol groups, the chi-6, and chi-6′ angles). However, energies were always very high whenever $\psi$ was close to 0°, regardless of the $\varphi$ value (Figs. 3 and 4) due to ring–ring steric interactions. In these runs, $\omega$ was always started at 180°, but it could relax as it was not a driven angle. Most of the structures having energies within 10 kcal mol$^{-1}$ of the minimum had $\psi$ values close to 180° (the antiperiplanar arrangement of the three linkage bonds). $\psi$ values near +90°

* SURFER; Golden Software, Golden, CO, 80402 U.S.A.

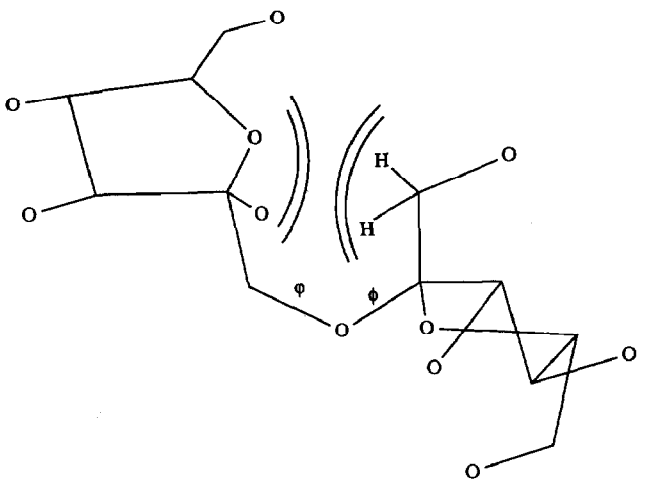


Fig. 3. Two-dimensional representation of the interactions occurring when $\varphi$ and $\psi$ are both 0°.

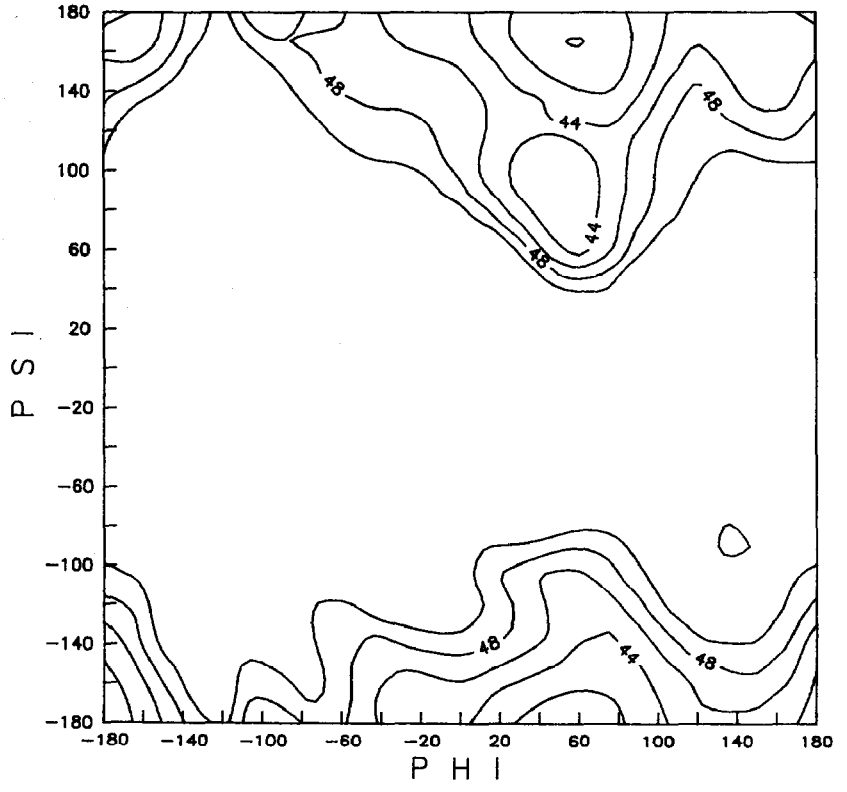


Fig. 4. Energy map from $\varphi$–$\psi$ run (A1). Values found on the contour levels indicate steric energies in kcal·mol$^{-1}$.

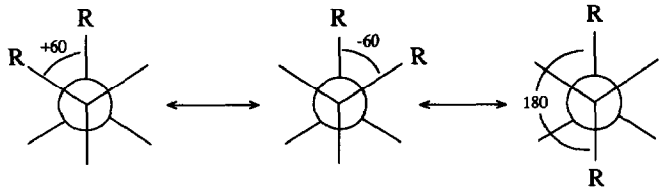


Fig. 5. Staggered conformations in a butane system.

gave energy values within 2–3 kcal·mol$^{-1}$ of the minimum for sharply limited ranges of $\varphi$. An analysis of this potential minimum was studied in run C6, but it did not produce any structures within 4 kcal·mol$^{-1}$ of the global minimum (Tables I, III, and IV.).

Those results suggested that conformations of **1** could be best understood by a $\varphi$–$\omega$ analysis. The $\psi$ angle would be started at an antiperiplanar angle and allowed to relax to the local minimum for each value of $\varphi$ and $\omega$. To a useful approximation, inulobiose molecules are butane derivatives with large terminal R-groups (Fig. 5). Only when the R-groups (five-membered rings) are antiperiplanar are they distant enough that the system has reasonable structural energy. This concept should apply to any system that contains rings linked by three bonds.

To test the general application of this proposal to simple five-membered rings, we carried out $\varphi$–$\omega$ conformational analyses on 1,2-dicyclopentylethane (**2**) (run B1) and 1,2-(1,1′-dimethyldicyclopentyl)ethane (**3**) (run B2) (Tables I and II). The torsion angle of the central bond was started at 180° and allowed to find the local minimum during optimizations of the entire structure at each increment of $\varphi$ and $\omega$. For most $\varphi$–$\omega$ values, the optimal value of $\psi$ was within 1.5°–2° (Table II) of the initial antiperiplanar conformation. Gauche conformations at the central linkage were also tested with **3** (run B3). $\psi$ was initially set at $+60°$, and $\varphi$ and $\omega$ were again stepped through 360° in 20° increments. In this analysis, all structures having an energy within 10 kcal·mol$^{-1}$ of the minimum had $\psi$ angles that were radically altered from the starting value. The gauche form had converted to antiperiplanar forms, clearly demonstrating the steric demands on the gauche form. The two rings tend to collide even without side groups, and it is therefore reasonable to focus on variation of $\varphi$ and $\omega$.

*Final $\varphi$–$\omega$ Analysis.* — In the $\varphi$–$\omega$ analyses, five initial combinations of side-group orientations and $\psi = +160°$ (C1–C5) were selected because they gave low energies in the A1–A9 series. The energy contours for the five runs were similar to C3 (Fig. 6). Energetic minima were found when $\varphi$ and $\omega$ were in nearly staggered conformations, but $\varphi$ values near $+60°$ gave lower energies than 180°, that were in turn much lower than $-60°$. High steric energy values when $\varphi = -60°$ result from conflicts with the $CH_2$ group of the linkage, OH on C-1′, and OH on C-3′. These interactions are minimized when chi-1′ is set to $-60°$ (run C2), but are not present when $\varphi = +60°$. Therefore, the lowest energies are found when $\varphi = +60°$.

There is a clearly favored angle for $\varphi$, but $\omega$-values of 180° gave energies only 2 kcal·mol$^{-1}$ higher than $\omega$ values near $-60°$, and the other staggered form (60°) was

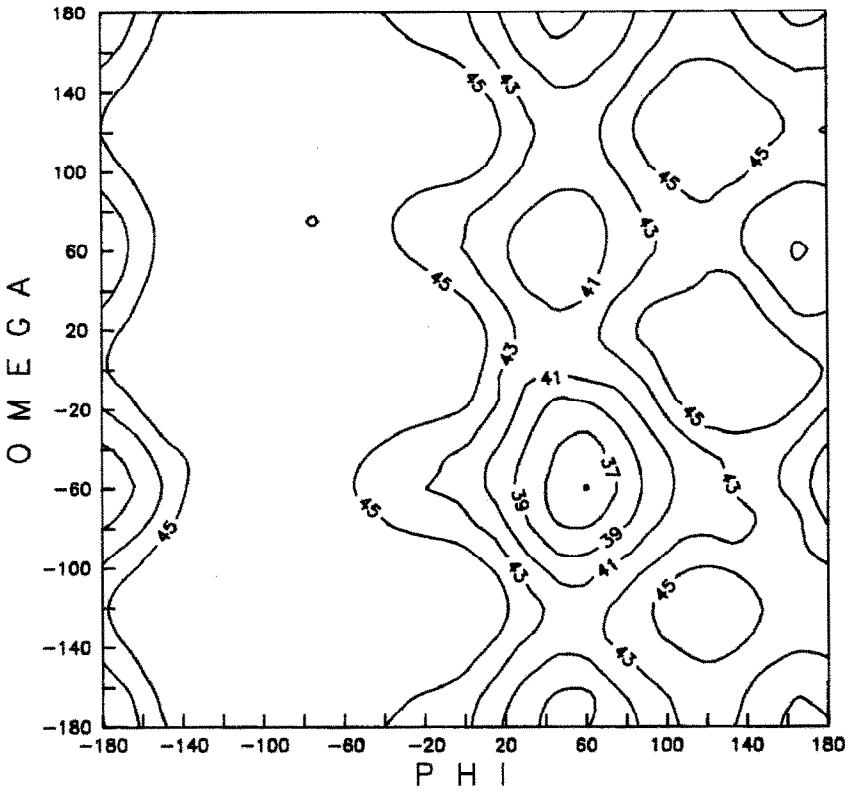


Fig. 6. Energy map from a $\varphi$–$\omega$ run (C3). Values found on the contour levels indicate steric energies in kcal·mol$^{-1}$.

within 4 kcal·mol$^{-1}$. As expected, the high energies occur at eclipsing angles of $\varphi$ and $\omega$ giving the map approximate threefold axes of symmetry in both dimensions.

The optimal values of $\varphi$ and $\omega$ were always the same, $+60°$ and $-60°$, respectively, regardless of the various positions tried for the primary alcohol groups (Tables III and IV). The lowest energies were found when the primary alcohols at C-5 and C-5′ had conformations near $-60°$ as found by French and Tran[13].

Table V reports which run gave the lowest energy at each $\varphi$–$\omega$ grid point. The least energetic result at most points was from run C3, but all runs except C1 contributed one or more values. At points where C3 did not furnish the least energetic model, the difference between it and the favored model was within 2.77 kcal·mol$^{-1}$ and usually smaller. On the other hand, some starting models resulted in structures that were almost 9 kcal·mol$^{-1}$ more energetic when C3 furnished the low-energy structure. The side group orientations of C3 were preferred overall, both because C3 led to the global minimum in energy and because it yielded the favoured structure at more points than the four other runs combined.

The structures at minima from each of the C series driver studies were re-optimized without any geometric restrictions, and there were small adjustments in some

torsion angles. It is interesting to compare the global minimum from C3 with the crystallographic structure of the inulobiose fragment in 1-kestose because $\varphi$ and $\psi$ are within the same staggered form, although $\varphi$ is very distorted, but $\omega$ is a completely different staggered form. Investigations of the 1-kestose structure, currently underway in this lab, should reveal the reason for the discrepancy.

*Variations in ring conformations.* — French and Tran[13] found two energy wells for fructofuranose ring puckering, a dominant one near the ${}^{4}_{3}T$ conformation ($\varphi_2 = 270°$), and a secondary one near the ${}^{3}_{4}T$ conformation ($\varphi_2 = 90°$) (Fig. 2). The models in this study started only with the ${}^{4}_{3}T$ structure from that work.

The Cremer–Pople angle of ring puckering was monitored during the $\varphi$–$\psi$ and $\psi$–$\omega$ analyses for the two rings of **1**. In the initial studies (runs A1–A9), when values of $\varphi$ and $\psi$ combined to give structures with high energies, the Cremer–Pople $\varphi_2$ angle varied over all possible values. When the energies were low, the rings stayed in conformations near the starting $\varphi_2$ of 265°.

In the $\varphi$–$\omega$ studies, there were no severe interactions, and the range of $\varphi_2$ for Fru-1 was 245–287° while it was 257–281° for Fru-2 (Fig. 1). This does not include any structure similar to the fructose ring in kestose which is near the ${}^{3}_{4}T$ conformation ($\varphi_2 = 90°$).

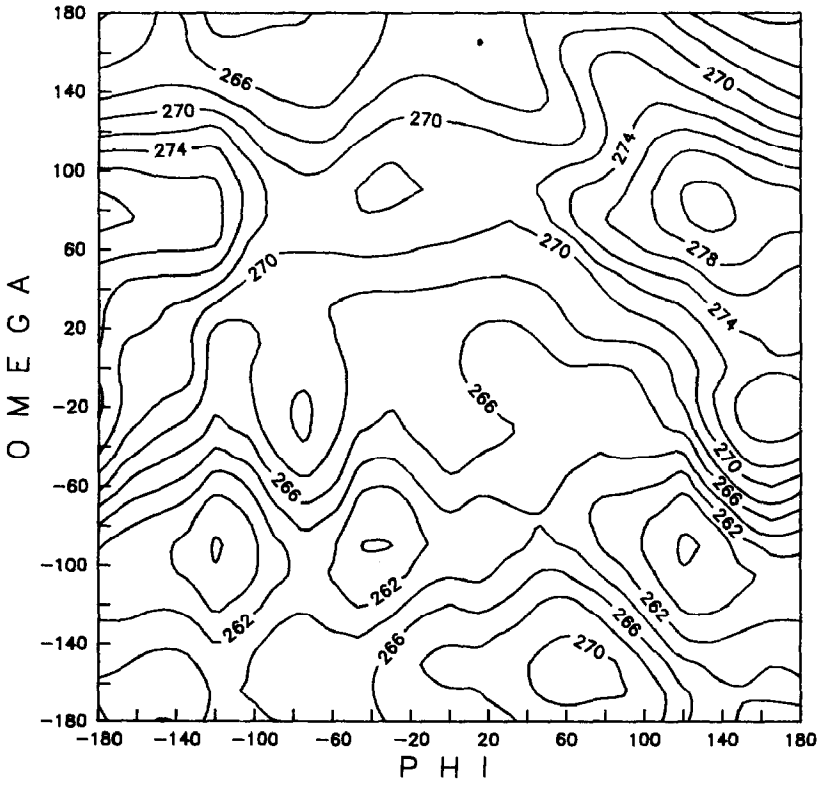


Fig. 7. Pseudorotation map for Fru-1 (Fig. 1). Values found on the contour levels indicate the Cremer–Pople phase angle of pseudorotation, $\varphi_2$.

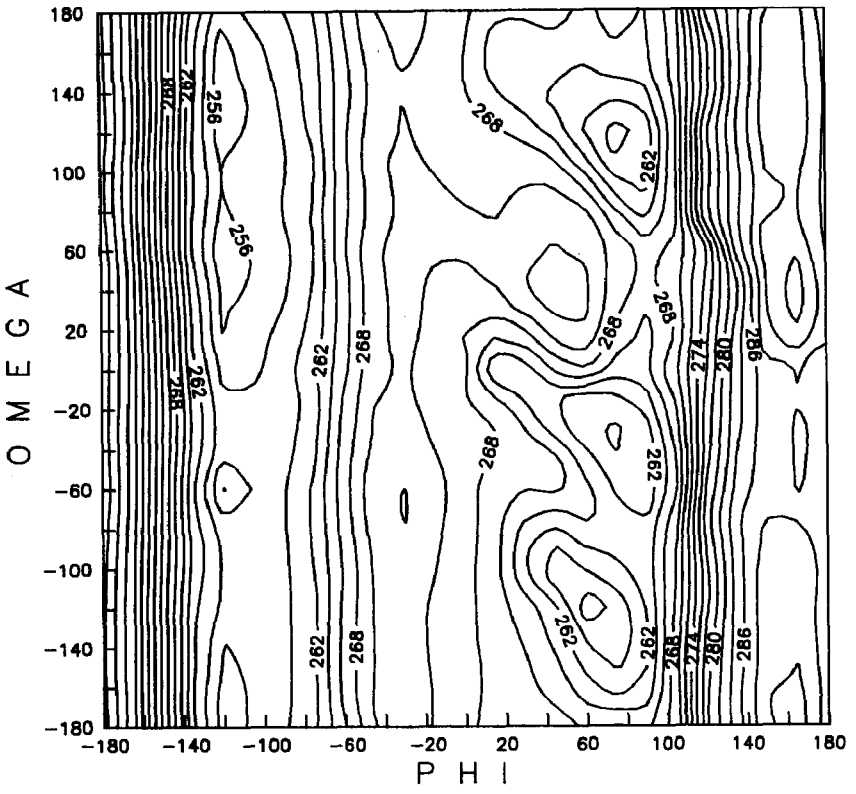


Fig. 8. Pseudorotation map for Fru-2 (Fig. 1).

The variations that were observed in $\varphi_2$ did correlate with changes in the linkage angle. In Fru-1, C-2 is part of the four-atom sequence that defines the $\omega$ angle, and when $\omega$ is varied, $\varphi_2$ of Fru-1 fluctuates. When $\varphi$ is varied there is negligible effect on Fru-1. The same effect is seen between Fru-2 and its linkage angles (Fig. 7 and Fig. 8 for data from run C3). Thus the amount of deviation is clearly related to the level of steric strain.

*Ψ Analysis.* — The antiperiplanar conformation of the three-bond linkage was the minimum energy angle found in all the systems analyzed in this work (Tables III and IV). This conformation is also found in X-ray diffraction analyses where the torsion angle of $\psi$ in the inulobiose moiety of 1-kestose[7] is $-162.34°$, and, in the levanbiose moiety of 6-kestose[17], it is 145.6°. In symmetrical systems like **2** and **3**, the rings are almost exactly antiperiplanar with one another. In unsymmetrical systems like **1** or levanbiose, the $\psi$ angle deviates from antiperiplanarity because side-groups affect the final conformation of the three-bond linkage. In **1**, for example, to minimize interactions between the $CH_2$ in the linkage and the -OH on C-3, $\psi$ relaxes to about 160°. Comparing runs C3 and C4, chi-6 and chi-6′ were set to $-60°$ and $+60°$, respectively. The average $\psi$ angle for run C3, was 165°, whereas in run C4, the average $\psi$ value obtained was 160°.

Other sugars with three-bond linkages have also been found to prefer a central torsion angle near 180°. A review by Jeffrey[18] lists such linkage torsion angles, and seven of the eight cases mentioned had $\psi$ angles of 156° or higher, and one case of 104°.

*Comparison of other computational methods with global minimum structure.* — The global minimum structure was subjected to re-minimization using other programs to see what differences might be observed in the structural geometry. Calculations were carried out with MM2P(87), MM3, and MOPAC(AM1). The results are listed in Table VI. Generally little effect was seen, confirming the accuracy of the methodology employed.

*Conclusions.* — This study underscores one of the unique values of computational modeling: the ability to study a compound which cannot be isolated in pure form. While a furanose dimer could provide much useful information towards understanding other compounds containing such a component, simple fructose oligomers generally adopt pyranose forms at the reducing end. Modeling can be used to study a furanose dimer, and provide information not available from experiments. The results found here will be helpful in understanding the conformations of other compounds which contain this linkage, including 1-kestose, now under investigation in this laboratory, and even the polymer inulin. A stereo view of the global minimum is shown in Fig. 9, and the coordinates are listed in Table VII.

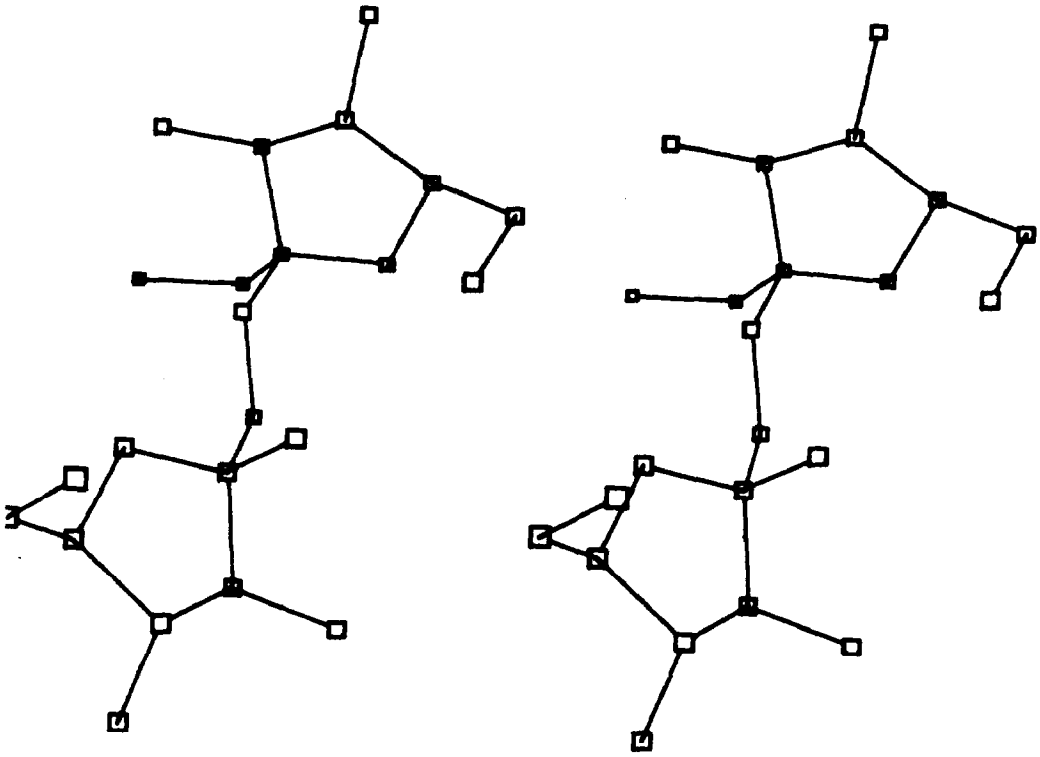

Fig. 9. Stereo drawing of the global minimum inulobiose structure.

TABLE VII

The coordinates of the global minimum structure from run C3 as shown in Fig. 9.

| *Atom* | x | y | z | *Atom* | x | y | z |
|---|---|---|---|---|---|---|---|
| C-1 | −0.01497 | 0.00283 | 0.03785 | H-1 | −0.40154 | −0.63113 | −0.79194 |
| C-2 | 1.5067 | −0.05088 | 0.03247 | H-1 | −0.38604 | −0.38705 | 1.01275 |
| C-3 | 2.08711 | −1.44109 | 0.23655 | H-3 | 1.50309 | −2.0046 | 1.00229 |
| C-4 | 3.47485 | −1.10703 | 0.74989 | H-4 | 4.1738 | −0.85113 | −0.08022 |
| C-5 | 3.14947 | 0.08822 | 1.63522 | H-5 | 2.80113 | −0.29052 | 2.62785 |
| C-6 | 4.29874 | 1.0584 | 1.86903 | H-6 | 3.9875 | 1.89196 | 2.54071 |
| | | | | H-6 | 5.16792 | 0.53166 | 2.32576 |
| O-5 | 2.04049 | 0.759 | 1.05222 | | | | |
| O-3 | 2.12436 | −2.22541 | −0.95486 | H-1′ | −3.79887 | 1.06434 | 0.38879 |
| O-4 | 4.02664 | −2.18173 | 1.50928 | H-1′ | −2.62817 | −0.27531 | 0.58298 |
| O-2 | 2.0197 | 0.49396 | −1.18003 | H-3′ | −3.17231 | 3.26118 | −0.36965 |
| O-6 | 4.74043 | 1.62939 | 0.63523 | H-4′ | −0.47755 | 3.50527 | −1.88658 |
| O-1–O2 | −0.43356 | 1.34905 | −0.12101 | H-5′ | −3.07234 | 2.24968 | −2.95539 |
| | | | | H-6′ | −1.56386 | 0.87683 | −4.36253 |
| C-1′ | −2.73148 | 0.83294 | 0.60926 | H-6′ | −1.11898 | 2.62625 | −4.53054 |
| C-2′ | −1.81405 | 1.54104 | −0.3824 | | | | |
| C-3′ | −2.08293 | 3.04197 | −0.47056 | OH-2 | 1.74955 | 1.39217 | −1.26765 |
| C-4′ | −1.58335 | 3.36206 | −1.8665 | OH-3 | 2.50341 | −1.72079 | −1.65476 |
| C-5′ | −2.01634 | 2.11311 | −2.61523 | OH-4 | 4.22126 | −2.89076 | 0.91937 |
| C-6′ | −1.15903 | 1.76522 | −3.82443 | OH-6 | 4.03511 | 2.13899 | 0.27213 |
| O-1′ | −2.45333 | 1.28794 | 1.93386 | OH-1′ | −3.07114 | 0.90046 | 2.53072 |
| O-5′ | −2.03284 | 1.04106 | −1.68534 | OH-3′ | −1.48533 | 3.42869 | 1.35031 |
| O-3′ | −1.36792 | 3.81031 | 0.49783 | OH-4′ | −1.88941 | 5.27567 | −1.91501 |
| O-4′ | −2.21137 | 4.53008 | −2.39352 | OH-6′ | 0.19127 | 0.60418 | −3.04724 |
| O-6′ | 0.18259 | 1.46627 | −3.42987 | | | | |

The distinctive features of the inulobiose structure include the three-bond linkage, the ring-puckering form, and the side-group orientations. It is useful to think of the inulobiose structure with three bonds linking the sugar rings as a butane-type system. When large groups, such as furanose rings, replace the terminal carbon atoms, structures with low energies will have an antiperiplanar angle at the central ($\psi$) bond. The other staggered forms of $\psi$ have very high steric strain. This hypothesis is corroborated by Jeffrey's review of crystallographic studies[18]. The other two linkage angles, $\varphi$ and $\omega$, can accommodate most staggered forms. In the global minimum, the rings are separated as far as possible. Because this separation leads to few inter-ring interactions, the individual ring units tend to adopt the least energetic forms found for the monomeric units, and that is observed here both with the ring puckering form, $\varphi_2$ and with orientation the side-groups.

On the other hand, inulobiose is a very flexible structure, and there are numerous linkage angles which are energetically accessible, and, given other constraints, these other angles will be preferred. This study correlates how the other structural features will change under those circumstances.

ACKNOWLEDGMENT

A Tulane Biomedical Research Support Grant provided partial support for this study.

REFERENCES

1 J. H. Pazur and A. L. Gordon, *J. Am. Chem. Soc.*, 75 (1953) 3458–3460.
2 B. Andersen, *Acta Chem. Scand.*, 21 (1967) 828–829.
3 J. H. Pazur, *J. Biol. Chem.*, 199 (1952) 217–225.
4 T. Adachi, T. Niizato, H. Hidaka, and U. Takeda, Ger. Offen. DE 3 232 531 (1981); *Chem. Abstr.*, 98 (1983) 530.
5 E. Middleton, *J. Membrane Biol.*, 34 (1977) 93–101.
6 A. Fuchs, *Stärke*, 39 (1987) 335–343.
7 G. A. Jeffrey and Y. J. Park, *Acta Crystallogr., Sect. B*, 28 (1972) 257–267.
8 A. D. French, *Carbohydr. Res.*, 176 (1988) 17–29.
9 R. H. Marchessault, T. Bleha, Y. Deslandes, and J.-F. Revol, *Can. J. Chem.* 58 (1980) 2415–2422.
10 A. French, *J. Plant Physiol.*, 134 (1989) 125–136.
11 T. M. Calub, A. L. Waterhouse, and A. D. French, unpublished results.
12 W. Saenger, *Principles of Nucleic Acid Structure*, Springer-Verlag, New York, 1984, p. 17.
13 A. D. French and V. Tran, *Biopolymers*, (1990), *in press.*
14 D. Cremer and J. A. Pople, *J. Am. Chem. Soc.*, 97 (1975) 1354–1355.
15 A. D. French, V. Tran, and S. Perez, in A.D. French and J.W. Brady (Eds.), *Computer Modeling of Carbohydrate Molecules*, ACS Symposium Series 430, American Chemical Society, Washington, DC, 1990, pp. 191–212.
16 L. Nørskov and N. L. Allinger, *J. Computational Chem.*, (1984) 326–335.
17 V. Ferretti, V. Bertolasi, and G. Gilli, *Acta Crystallogr., Sect. C*, 40 (1984) 531–535.
18 G. A. Jeffrey, *Acta Crystallogr., Sect. B*, 49 (1990), 89–103.